Treatment of relapsing paralysis in experimental encephalomyelitis by targeting Th1 cells through atorvastatin

Aktas, O. and Waiczies, S. and Smorodchenko, A. and Dorr, J. and Seeger, B. and Prozorovski, T. and Sallach, S. and Endres, M. and Brocke, S. and Nitsch, R. and Zipp, F.

This is a copy of the final article, which was first published online on 10 March 2003 and in final edited form in:

Journal of Experimental Medicine
2003 MAR 17 ; 197(6): 725-733
doi: 10.1084/jem.20021425

Publisher: Rockefeller University Press

Published March 10, 2003

Treatment of Relapsing Paralysis in Experimental Encephalomyelitis by Targeting Th1 Cells through Atorvastatin

Orhan Aktas,[1] Sonia Waiczies,[1] Alina Smorodchenko,[1] Jan Dörr,[1] Bibiane Seeger,[1] Timour Prozorovski,[1] Stephanie Sallach,[2] Matthias Endres,[3] Stefan Brocke,[4] Robert Nitsch,[2] and Frauke Zipp[1]

[1]*Institute of Neuroimmunology, Neuroscience Research Center,* [2]*Department of Cell and Neurobiology, Institute of Anatomy, and* [3]*Department of Neurology, Charité, Humboldt University, 10098 Berlin, Germany*
[4]*Department of Pathology, Hebrew University Hadassah Medical School, Jerusalem 91120, Israel*

Abstract

Statins, known as inhibitors of 3-hydroxy-3-methylglutaryl coenzyme A (HMG-CoA) reductase, exhibit numerous functions related to inflammation, such as MHC class II down-regulation, interference with T cell adhesion, and induction of apoptosis. Here we demonstrate that both subcutaneous and oral administration of atorvastatin inhibit the development of actively induced chronic experimental autoimmune encephalomyelitis in SJL/J mice and significantly reduce the inflammatory infiltration into the central nervous system (CNS). When treatment was started after disease onset, atorvastatin reduced the incidence of relapses and protected from the development of further disability. Both the reduced autoreactive T cell response measured by proliferation toward the encephalitogenic peptide PLP139–151 and the cytokine profile indicate a potent blockade of T helper cell type 1 immune response. In in vitro assays atorvastatin not only inhibited antigen-specific responses, but also decreased T cell proliferation mediated by direct TCR engagement independently of MHC class II and LFA-1. Inhibition of proliferation was not due to apoptosis induction, but linked to a negative regulation on cell cycle progression. However, early T cell activation was unaffected, as reflected by unaltered calcium fluxes. Thus, our results provide evidence for a beneficial role of statins in the treatment of autoimmune attack on the CNS.

Key words: EAE • multiple sclerosis • HMG-CoA reductase • T cell • autoimmunity

Introduction

Several large-scale intervention trials have demonstrated that statin treatment reduces the risk of myocardial infarction and stroke (1). This effect was so far explained by their impact on the lipid profile through the inhibition of an enzyme crucial to cellular cholesterol synthesis, 3-hydroxy-3-methylglutaryl coenzyme A (HMG-CoA)* reductase. However, increasing clinical and experimental evidence suggests that the pharmacological effects of statins relate not only to cholesterol lowering but also to anti-inflammatory effects on the immune system. Two independent studies have shown that both pravastatin and lovastatin reduce serum concentrations of C-reactive protein, a marker of inflammation, by ~15% (2, 3). In addition, clinical trials on transplant rejections indicate the therapeutic potential of statins as immunosuppressive agents. For example, pravastatin improves survival and lowers the incidence of acute rejection after heart transplantation (4). Concerning the underlying mechanisms, Kwak et al. demonstrated in an initial report that statins inhibit the IFN-γ–induced expression of MHC class II on most APCs, including B cells and macrophages (5). A recent paper showed that certain statins inhibit the LFA-1–dependent stimulation of T cells and that a lovastatin-based LFA-1 inhibitor reduces infiltration of neutrophils in the murine thioglycollate-induced peritonitis model (6). Members of the statin family were found to

Address correspondence to Frauke Zipp, Institute of Neuroimmunology, Neuroscience Research Center, NWFZ 2680, Charité, 10098 Berlin, Germany. Phone: 149-30-450-539028; Fax: 149-30-450-539906; E-mail: frauke.zipp@charite.de

**Abbreviations used in this paper:* BP, birch pollen; CDK, cyclin-dependent kinase; CNS, central nervous system; EAE, encephalomyelitis; HMG-CoA, 3-hydroxy-3-methylglutaryl coenzyme A; ICAM-1, intercellular adhesion molecule-1; MBP, myelin basic protein; MS, multiple sclerosis; PLP, proteolipid protein; TCL, T cell line.

 J. Exp. Med. © The Rockefeller University Press • 0022-1007/2003/03/725/9 $8.00
Volume 197, Number 6, March 17, 2003 725–733
http://www.jem.org/cgi/doi/10.1084/jem.20021425

Published March 10, 2003

interfere with the LFA-1–intercellular adhesion molecule (ICAM)-1 interaction by binding to a novel regulatory site of integrins in a HMG-CoA–independent manner. These observations raise the question as to whether statin therapy may also be beneficial in other chronic inflammatory conditions and immune diseases (7).

In this report, we used the pharmacologically active statin atorvastatin to dissect the role of statins in brain inflammation and to explore their therapeutic potential for autoimmunity. Therefore, we applied atorvastatin in murine experimental autoimmune encephalomyelitis (EAE; reference 8), a well-characterized $CD4^+$ T cell–mediated animal disease model of multiple sclerosis (MS; references 9, 10). As for its human counterpart, induction of EAE in susceptible strains of rodents leads to central nervous system (CNS) inflammation, demyelination, and axonal pathology (11). We demonstrate that the signs of relapsing–remitting EAE in SJL/J mice can be diminished by atorvastatin in vivo both in a preventive and therapeutic fashion. CNS inflammation associated with EAE was significantly reduced. Our data indicate that this therapeutic effect is caused by a down-regulation of Th1 immune response, as confirmed by the reduction of autoreactive T cell response and infiltration into the CNS. We further demonstrate an HMG-CoA-reductase–dependent interference of atorvastatin with the cell cycle in human antigen–specific T cells.

Materials and Methods

Treatment with Atorvastatin and Mevalonate. Because pure atorvastatin (Pfizer) is not soluble in PBS, the stock was dissolved in 2% DMSO before subcutaneous administration at a daily dose of 20 or 200 μg per mouse (corresponding to 1 or 10 mg/kg body weight) and in methylcellulose 0.5% (Sigma-Aldrich) before oral administration of 200 μg per mouse (10 mg/kg) for the in vivo experiments. Accordingly, the in vitro investigations were performed at a concentration of 1, 5, and 25 μM of atorvastatin (100 μM stock in 2% DMSO). In all assays of our work, the carrier was used as vehicle control in the same dilution as atorvastatin. To test the reversibility of the atorvastatin effect, L-mevalonate was used at a concentration of 200 μM. Therefore, L-mevalonic acid lactone (Sigma-Aldrich) was activated by 1 N NaOH. The resulting solution was neutralized with 1 N HCl to pH 7.2, diluted with distilled water, and sterilized by filtration thereafter.

Induction, Treatment, and Clinical Evaluation of Active EAE. Female SJL/J mice (6–8 wk; ~20 g body weight; Charles River Laboratories) were immunized subcutaneously with 75 μg proteolipid protein (PLP) 139–151 (purity >95%; Pepceuticals) in 0.2 ml emulsion consisting of equal volumes of PBS and CFA (Difco) and containing 6 mg/ml of mycobacterium tuberculosis H37Ra (Difco). 200 ng pertussis toxin (List Biological Laboratories) was administered intraperitoneally at days 0 and 2 (12). Mice were scored for EAE as follows: 0, no disease; 1, tail weakness; 2, paraparesis; 3, paraplegia; 4, paraplegia with forelimb weakness or paralysis; and 5, moribund or dead animals (13). Mean clinical scores at separate days and mean maximal scores were calculated by adding scores of individual mice and dividing by number of mice in each group. All procedures were conducted according to protocols approved by the local animal welfare committee.

Neuropathology. Mice killed with narcotics were transcardially perfused with 4% paraformaldehyde. Spinal cords and brain stems were removed, postfixed in 4% paraformaldehyde, and embedded in paraffin. Vibratome sections (Shandon) were stained with hematoxylin and eosin for visualization of inflammatory infiltrates and evaluated in a blinded manner for the amount of inflammation as described previously (14).

Human and Murine Antigen-specific T Cells. Human $CD4^+$ T cell lines (TCLs) specific for human myelin basic protein (MBP; MA14) or birch pollen (BP; MB7, MB8, EG8) were established with a modified "split-well" protocol (15) and have been characterized previously (16). All antigen-specific TCLs had at least three restimulations before the assay and a stimulation index >3. Establishment of the PLP139–151-specific mouse TCL Je1 was performed as described previously (17). For murine bulk cell cultures, spleen and draining lymph node cells were dissociated with a cell strainer (Sigma-Aldrich) and cultured in 96- (for proliferation assays) or 24-well microtiter plates (for cytokine assays).

Proliferation and Cytokine Assays. For the proliferation of human TCLs, 0.7×10^5 cells were stimulated with 2×10^5 autologous-irradiated (3,000 rad) PBMC as antigen-presenting cells and the corresponding antigen, or with anti-CD3 (OKT3; coated at 1 μg/ml; American Type Culture Collection) and 1 μg/ml anti-CD28 (R&D Systems). For the proliferation of the mouse PLP139–151-specific TCL Je1, 0.7×10^5 cells were stimulated with 1.4×10^5 autologous-irradiated (3,000 rad) splenocytes as APC and 5 μg/ml peptide. For proliferation assays, [^{3}H]Thymidine (0.5 μCi per well; Amersham Biosciences) incorporation was measured 72 h after stimulation with antigen and 48 h with anti-CD3/CD28, radioactivity as counts per minutes detected by a MicroBeta® β counter (PerkinElmer) after 18 h. For the ex vivo proliferation and cytokine measurement, 2×10^6 splenocytes were stimulated with different peptide concentrations. Human IFN-γ and mouse IL-2, IL-12, IFN-γ, IL-4, and IL-10 were measured in supernatants from cell cultures (2×10^6/ml in 24-well plates; incubation time 48 h for IL-2, IL-12, and IFN-γ; 96 h for IL-4 and IL-10) with commercially available sandwich ELISA® kits (mouse, BD Biosciences; human, R&D Systems).

Western Blot. Immunoblot studies were performed as described previously (16). In brief, after 2-h blocking, membranes were incubated for 1 h with specific primary antibodies: 2 μg/ml monoclonal mouse anti-$p27^{Kip1}$ (Santa Cruz Biotechnology, Inc.), 1 μg/ml polyclonal rabbit anti-CDK4 (Santa Cruz Biotechnology, Inc.), and 24 ng/ml monoclonal anti–β-actin. Membranes were incubated for 1 h with 1.25 μg/ml secondary antibody coupled to horseradish peroxidase (DakoCytomation). Specific bands were detected with the ECL-Plus™ System (Amersham Biosciences). CDK4 and $p27^{Kip1}$ immunoblots were sequentially incubated with anti–β-actin as control.

Measurements of Intracellular Calcium $[Ca^{2+}]_i$. Intracellular free calcium concentrations $[Ca^{2+}]_i$ were measured in human TCLs using flow cytometry (18). Cells, 5×10^6/ml, were loaded with 5 μM Indo-1-AM (Molecular Probes) for 30 min at 37°C. Unloaded dye was removed by centrifugation, and cells were resuspended in calcium-free PBS. The analyses were performed on a flow-activated cell sorter (BD FACS® LSR; Becton Dickinson). The FL4 (510/20) and FL5 (380LP) fluorescence channels were used to measure free Indo-1 and the complex Ca^{2+}–Indo-1 concentrations, respectively. Calculation

Published March 10, 2003

of the ratio of these two fluorescent wavelengths allows the evaluation of changes in cytosolic-free Ca^{2+} concentrations $[Ca^{2+}]_i$ independently of the cell size and the intracellular Indo-1 concentration. The flow rate was set to 300 events/s and the mean ratio of 2,000 cells were noted every 20 s. 5 μM Tg (Calbiochem) was added after 80 s to fully deplete intracellular Ca^{2+} stores and therefore activate calcium release-activated calcium channels (CRACs). After a 5-min incubation with Tg, 1.2 mM calcium was added to the cell suspension to monitor the extent of Ca^{2+} influx.

Apoptosis Assay. DNA fragmentation of apoptosis-susceptible Jurkat T cells was determined as described previously (15). 2×10^5 cells were incubated with atorvastatin or vehicle at the indicated concentrations. As a positive control, CD95-mediated apoptosis was induced by a soluble murine CD95 ligand. After 24 h, cells were washed and incubated overnight at 4°C in a hypotonic fluorochrome solution containing 50 μg/ml propidium iodide before flow cytometry for quantitative detection of hypodiploid DNA.

Statistics. For group comparisons (mean maximal disease scores and number of inflammatory foci in spinal cord), the Student's *t* test was applied. To compare the EAE courses, statistical analysis of repeated measurements was performed by analysis of variance using the Fisher's pairwise least significant difference test with Bonferroni adjustment (19). The incidence of relapses (defined as the acquisition of a clinical score >1 for at least two consecutive days; modified according to reference 20) was compared using the χ^2 test.

Results and Discussion

Atorvastatin Ameliorates Disease Severity in EAE. To explore the efficacy of statins on actively induced EAE, PLP139–151-immunized SJL/J mice were treated subcutaneously with 200 μg per mouse (corresponding to 10 mg/kg body weight) atorvastatin (all treatments using pure substance) from day 1 after immunization. This dosage was chosen in accordance with previous work on statin effects in murine lipid metabolism (21–23) and stroke models (24, 25), assuming that mouse and man greatly differ in their statin metabolism (26–29). Preventive treatment attenuated the first disease attack and reduced clinical symptoms (Fig. 1 A), resulting in a reduced mean maximum disease score of 2.4 ± 0.3 (mean ± SEM) in the atorvastatin group versus 3.4 ± 0.3 in the vehicle group (data from two independent experiments; $n = 12$ for both groups; $P < 0.05$). Continued atorvastatin therapy of these animals significantly protected them from the development of long-term neurological sequelae, as the mean clinical scores between groups were statistically different ($F_{14–70}$ [1, 57] = 4.4, $P < 0.05$). This marked prophylactic effect of atorvastatin led us to investigate its therapeutic potential to suppress established disease. Hence, we delayed starting treatment with atorvastatin until animals developed the first symptoms. Treatment with atorvastatin prevented mice from disease exacerbation with a relapse rate of 37.5% (three out of eight) in the atorvastatin group compared with 87.5% (seven out of eight) in the vehicle group ($\chi^2 = 4.3$; $P < 0.05$). Neurological disability during relapse was reduced (Fig. 1 B) with a maximum disease score of 1.2 ± 0.4 in the atorvastatin group versus 2.4 ± 0.4 in the vehicle group ($P < 0.05$), and significantly lower mean

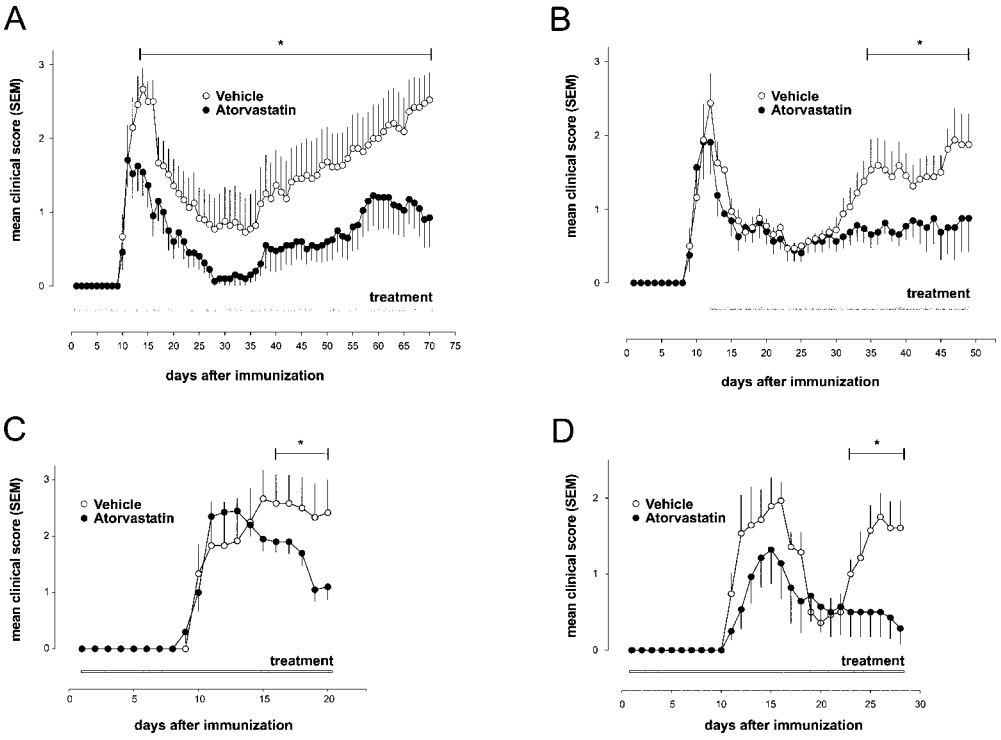

Figure 1. Atorvastatin suppresses the clinical severity of EAE in a preventive and therapeutic manner. (A) For the preventive treatment paradigm, 200 μg atorvastatin ($n = 12$; shaded circles) or vehicle alone ($n = 12$; open circles) were injected subcutaneously daily from the day of immunization onward. Both the maximum disease scores and the mean clinical disease scores were significantly reduced in the atorvastatin group. (B) For the nonpreventive therapy, mice were randomized into two groups ($n = 8$ for both groups) after the establishment of disease at day 10 and subsequently treated. Significant differences were noted for the maximum disease scores, the relapse incidence, and the mean disease scores for the time of the relapse. (C) Mice were treated subcutaneously with 20 μg atorvastatin ($n = 10$ for atorvastatin group, $n = 7$ for vehicle group). (D) For oral therapy, mice were treated with 200 μg ($n = 7$ for both groups). For all trials, treatment periods are indicated by horizontal hatched bars. The treatment effect was statistically significant as outlined in the marked range for all presented EAE courses (*, $P < 0.05$, analysis of variance).

Published March 10, 2003

clinical disease scores ($F_{35–50}$ [1, 15] = 4.7; $P < 0.05$). The lower dose of 20 μg per mouse atorvastatin was less effective ($F_{18–20}$ [1, 3] = 5.1; $P < 0.05$; Fig. 1 C). Treatment with orally administered atorvastatin (200 μg per mouse) exhibited a beneficial effect in the same model ($F_{25–28}$ [1, 4] = 4.8; $P < 0.05$; Fig. 1 D). Our observations provide evidence that the HMG-CoA-reductase inhibitor atorvastatin has marked therapeutic effects on chronic relapsing-remitting autoimmune encephalomyelitis in SJL/J mice. Clinical disease in atorvastatin-treated mice was considerably milder compared with vehicle-treated controls, as displayed by reduced maximal disease severity and favorable long-term outcome. Moreover, therapy with atorvastatin was beneficial even when started after disease manifestation, indicating a role for therapy of an already established autoimmune disorder.

Histological examination of mice killed directly after the maximum of the relapse revealed large inflammatory lesions scattered throughout the brain stem and spinal cord in vehicle-treated mice, whereas those treated with the statin revealed significantly less inflammation (Fig. 2). Thus, in line with the clinical scores, we found that atorvastatin treatment resulted in reduced CNS inflammation. Taking the reported almost pleiotropic effects of the statins into account, possible explanations for these data are either a decrease in peripheral immune response or reduced transmigration into the CNS. Therefore, we addressed the mechanisms underlying the atorvastatin-mediated blockade of neuroinflammation.

Atorvastatin Treatment Inhibits T Cell Response in EAE. First, we examined the T cell response resulting from statin treatment in EAE, which was investigated after 10 d of treatment in cells from spleens exposed to the encephalitogenic PLP139–151 epitope. As shown in Fig. 3 A, mice treated with atorvastatin revealed a lower proliferative response after antigenic challenge, compared with vehicle-treated animals. In line with previous reports (25), treatment of normocholesterolemic SJL/J mice with atorvastatin for 10 d in contrast to therapy over several months did not alter serum cholesterol levels, with 57.3 ± 2.9 versus 55.7 ± 1.2 mg/dl in atorvastatin- versus vehicle-treated mice, respectively (mean ± SEM).

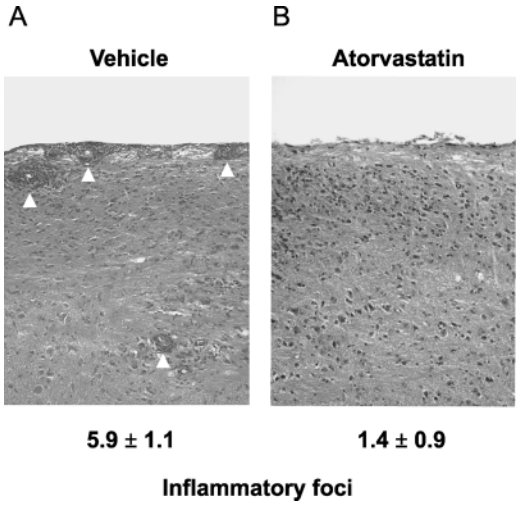

Figure 2. Decreased inflammation in spinal cords of atorvastatin-treated mice. Representative histology of spinal cord longitudinal sections was obtained from the EAE course presented in Fig. 1 A. Inflammatory infiltration was visualized by hematoxylin and eosin staining. (A) Vehicle-treated animals showed typical perivascular infiltrates (arrowheads) comprised of lymphocytes and macrophages. (B) In contrast, atorvastatin-treated animals showed a markedly reduced inflammatory reaction. Average number of inflammatory foci/ocular field ± SEM in spinal cords of atorvastatin- and vehicle-treated mice as detected in hematoxylin and eosin–stained sections ($P < 0.01$, Student's *t* test).

Inhibition of the Th1 Response by Atorvastatin in EAE. Assessment of the cytokine pattern in response to PLP restimulation indicated that atorvastatin treatment led to a reduction of IL-2 and IL-12 as well as IFN-γ secretion, as demonstrated for splenocyte cultures (Fig. 3, B–D). Interestingly, although immune cells from atorvastatin-treated animals showed a diminished proliferative response toward PLP, the levels of IL-4 and IL-10 in the supernatants of splenocytes were even higher on atorvastatin treatment, as compared with vehicle-treated animals (Fig. 3, E and F). IL-12 drives the T cell differentiation toward the Th1, and IFN-γ is a proinflammatory cytokine, possibly involved in the initiation of exacerbations in relapsing-remitting MS (30). In EAE, IFN-γ directs trafficking of leukocytes into the CNS by orchestrating chemokine production (31), and its overproduction is usually associated with relapses (32). Thus, inhibition of proliferation, IL-12, and IFN-γ production points to an antiinflammatory activity of atorvastatin, which accounts for the reduction of clinical disease. Our results demonstrate that atorvastatin is an effective immunomodulatory agent for the treatment of murine EAE by suppressing disease-causing Th1 response while enhancing regulatory cytokines. Clinical trials may clarify whether the same effects can be achieved in MS patients.

Decreased Proliferation of Murine and Human Lymphocytes Associated with Interference in Cell Cycle Regulation. In view of the reduced proliferative response in atorvastatin-treated animals, we investigated whether this statin interferes with the antigen-specific proliferation of a murine $CD4^+$ Th1 PLP-specific TCL Je1 in vitro. As shown in Fig. 4 A, atorvastatin blocked the antigen-response in a dose-dependent manner. The doses of 1–25 μM atorvastatin used in these assays are comparable to the levels measured in human plasma (29, 33). Having demonstrated the inhibitory effects of atorvastatin on murine cells in vivo and in vitro, we next studied the proliferation of human antigen-specific $CD4^+$ TCLs. As indicated in Fig. 4 B, antigen-specific proliferation of the human TCL MB8 was suppressed by atorvastatin in a dose-dependent manner.

Interestingly, the blockade of proliferation was also observed when atorvastatin was added to proliferating T cells, 24 or 48 h after stimulation (Fig. 5 A). This points to further pathways of immunomodulatory statin function in addition to those involving a reduced MHC class II upregulation by inhibition of the inducible promoter IV of the transactivator CIITA (5), and the blockade of LFA-1–

Published March 10, 2003

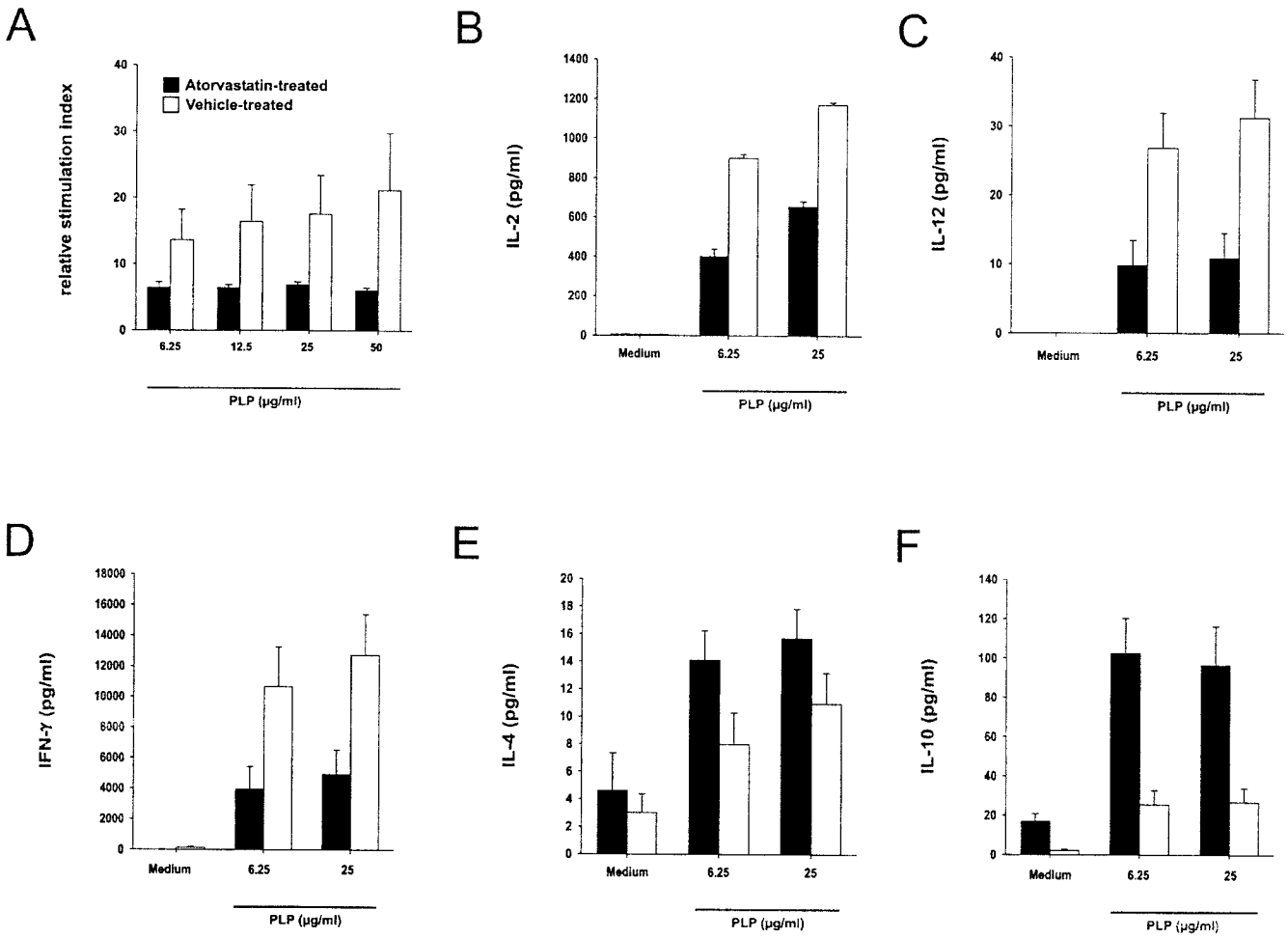

Figure 3. Atorvastatin treatment in vivo suppresses the PLP-specific priming response. Three mice per group were treated with either atorvastatin (200 μg per mouse) or vehicle from day 1 after immunization with PLP as described in Materials and Methods. (A) Proliferation of splenocytes in response to PLP (at the indicated concentrations) was assessed in quadruplicate cultures and expressed as stimulation index (mean ± SEM; atorvastatin, shaded bars; vehicle, open bars). (B) Accordingly, IL-2 was determined in the supernatants. Whereas IL-12 (C) as well as IFN-γ (D) were found at lower concentrations in the atorvastatin-treated mice than in those vehicle-treated, levels of IL-4 (E) and IL-10 (F) were higher in supernatants from splenocytes after treatment with atorvastatin. Data are presented as mean ± SEM; differences between atorvastatin and vehicle treatment are significant ($P < 0.05$; Student's *t* test).

ICAM-1 interactions (6). To confirm this hypothesis, we tested the ability of atorvastatin to block T cell proliferation in response to direct T cell receptor engagement independent of antigen presentation. As shown in Fig. 5 B, [^{3}H]Thymidine uptake of the antigen-specific TCL MB7 stimulated with anti-CD3/CD28 was markedly suppressed by atorvastatin. Thus, in an environment lacking APC, expressing MHC class II and ICAM-1, atorvastatin is nonetheless capable of inhibiting proliferation. Costimulation via T cell–mounted LFA-1 needs the addition of ICAM-1 not expressed on the T cell itself because direct T cell stimulation via CD3–TCR pathway alone does not induce phosphatidylinositol 3-kinase activation, a reliable indicator of costimulation mediated through ICAM-1 into the T cell (34). Therefore, a down-regulation of LFA-1 expression resulting in attenuated transmigration of mononuclear cells into the CNS (35), as well as ligation to the novel LFA-1 binding site as demonstrated by Weitz-Schmidt et al. (6), is not sufficient to explain the antiproliferative effect of atorvastatin in our CD3/CD28-stimulated T cells.

Reversibility of Atorvastatin-induced Interference with T Cell Proliferation and IFN-γ Secretion by L-Mevalonate. Because atorvastatin may confer its immunomodulatory effects, both dependent on (5) and independent of (6) inhibition of HMG-CoA reductase, it was important to clarify whether the direct T cell–targeted antiproliferative effect reported here is mediated by the HMG-CoA reductase pathway. Indeed, both proliferation (Fig. 5 B) and IFN-γ secretion (Fig. 5 C) in human antigen–specific T cells could be reversed by L-mevalonate providing direct evidence that the immunomodulatory effects of atorvastatin are mediated by inhibition of HMG-CoA reductase.

Impact of Atorvastatin on Cell Cycle Regulation. Because statins block the synthesis of isoprenoid intermediates and subsequently inhibit the function of intracellular signaling

Published March 10, 2003

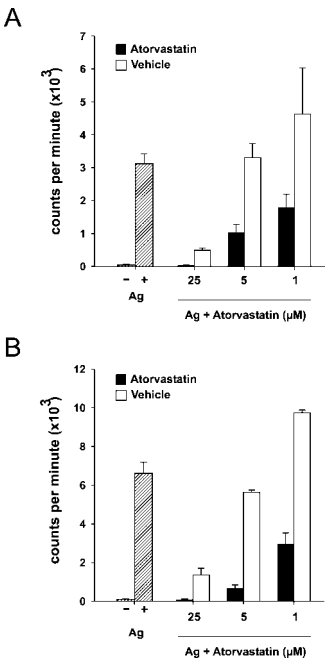

Figure 4. Atorvastatin inhibits antigen-dependent proliferation of murine and human TCLs. The murine CD4+ PLP-specific TCL Je1 (A) and the human BP-specific TCL MB8 (B) were stimulated with (+) or without (−) antigen presented by irradiated autologous APC in the absence or presence of different concentrations of atorvastatin (shaded bars) or vehicle alone (open bars), and proliferation was assessed. Striped bars correspond to controls without atorvastin or vehicle.

molecules (36), next we tested whether the observed antiproliferative effect of atorvastatin is caused by interference at the cell cycle level. We did not find an impact of atorvastatin on early T cell activation, because calcium influx was unaffected (Fig. 5 D). However, we could observe that growth inhibition by atorvastatin was associated with a down-regulation of the cyclin-dependent kinase 4 (CDK4; Fig. 5 E). Investigating the expression of $p27^{kip1}$, a CDK inhibitor involved in negative regulation of the T cell cycle, we found an up-regulation on atorvastatin incubation, which could be reversed by L-mevalonate (Fig. 5 F). This finding, together with a persisting effect of atorvastatin, even when added late in culture (Fig. 5 A), suggests an inhibition of cell cycle progression at the late part of the G1 phase.

No Induction of Apoptosis in T Cells by Atorvastatin. Principally, atorvastatin may not only inhibit but also directly eliminate cells by induction of apoptotic mechanisms (37). Testing statin-incubated T cells with the trypan blue exclusion assay, we had no indication of increased cell death. To exclude an apoptosis-inducing capacity of atorvastatin in T cells, which might be responsible for the antiproliferative effect, we measured DNA fragmentation. However, atorvastatin did not induce relevant DNA fragmentation, even in apoptosis-susceptible Jurkat T cells, compared with both untreated and vehicle-treated cells (Fig. 5 G), thus ruling out a proapoptotic role for this substance.

Disease pathogenesis in EAE induced by PLP139–151 in SJL/J mice is regarded as a prototypical T cell–mediated autoimmune disorder. As in MS, it involves the activation and expansion of autoreactive T cells, migration through the blood–brain barrier, restimulation by antigen challenge within the CNS, and induction of local inflammation, leading to demyelination and axonal damage. The reduced amount of inflammatory infiltration in the CNS from statin-treated mice might reflect the inhibition of T cell entry into the CNS. This hypothesis is supported by the fact that certain statins were capable of inhibiting thioglycollate-induced neutrophil migration (6). However, our data on the suppression of Th1 immune response outside the brain and the lack of the statin-binding site in the integrin very late antigen-4 (6), which is important for the transmigration through the blood–brain barrier, argue against a prominent impact of statins on T cell migration into the CNS. Thus, the reduced amount of inflammation in the CNS of statin-treated animals in our work most likely results from an effect on the peripheral immune response. In fact, in line with Youssef et al. (38), we found a diminished proliferative response of $CD4^+$ lymphocytes toward the encephalitogenic peptide PLP139–151, accompanied by reduced production of Th1 cytokines and a relative increase in the regulatory cytokines IL-4 and IL-10. It is striking that even the addition of the statin at a late stage of T cell activation resulted in a marked decrease of proliferation. This finding indicates that the immunomodulatory effects of atorvastatin are comprised of other mechanisms in addition to down-regulation of MHC class II expression and inhibition of LFA-1–ICAM-1 interaction.

Investigations in the murine system indicate that statins exert pleiotropic immunomodulatory effects on both APC and T cells (38). In line with previous observations on lovastatin and B cells (39), the antiproliferative effect of atorvastatin examined in human antigen-specific T cells in our work was not preceded by a reduced T cell activation because calcium influx was unaffected. Furthermore, this effect was not linked to the induction of apoptosis. Our data indicate that the underlying mechanism for the inhibition of T cell response in autoimmune neuroinflammation is the interference with cell cycle regulation represented by down-regulation of CDK4 and up-regulation of $p27^{kip1}$, which was reported previously as mechanism of action of statins only in mesangial cells (40). Immunological studies within clinical trials might finally clarify which atorvastatin-mediated mechanism is important in case of a beneficial effect in MS.

Via blocking HMG-CoA reductase and mevalonate synthesis, statins prevent the synthesis of important isoprenoid intermediates of the cholesterol biosynthetic pathway, which are important for isoprenylation of certain cell-signaling proteins (36). Thus, this posttranslational modification of intracellular signaling molecules, such as small GTP-binding proteins by isoprenylation (36), is involved in the regulation of the cell cycle by statins. Small GTP-binding proteins (e.g., Ras and Rho) require such posttranslational modification for membrane localization and activity and are implicated in cell cycle regulation. Among these proteins, Ras promotes cell cycle progression via activation of the mitogen-activated protein kinase pathway (41), whereas Rho causes cellular proliferation possibly through destabilizing $p27^{kip1}$ protein (42). In fact, we could

Published March 10, 2003

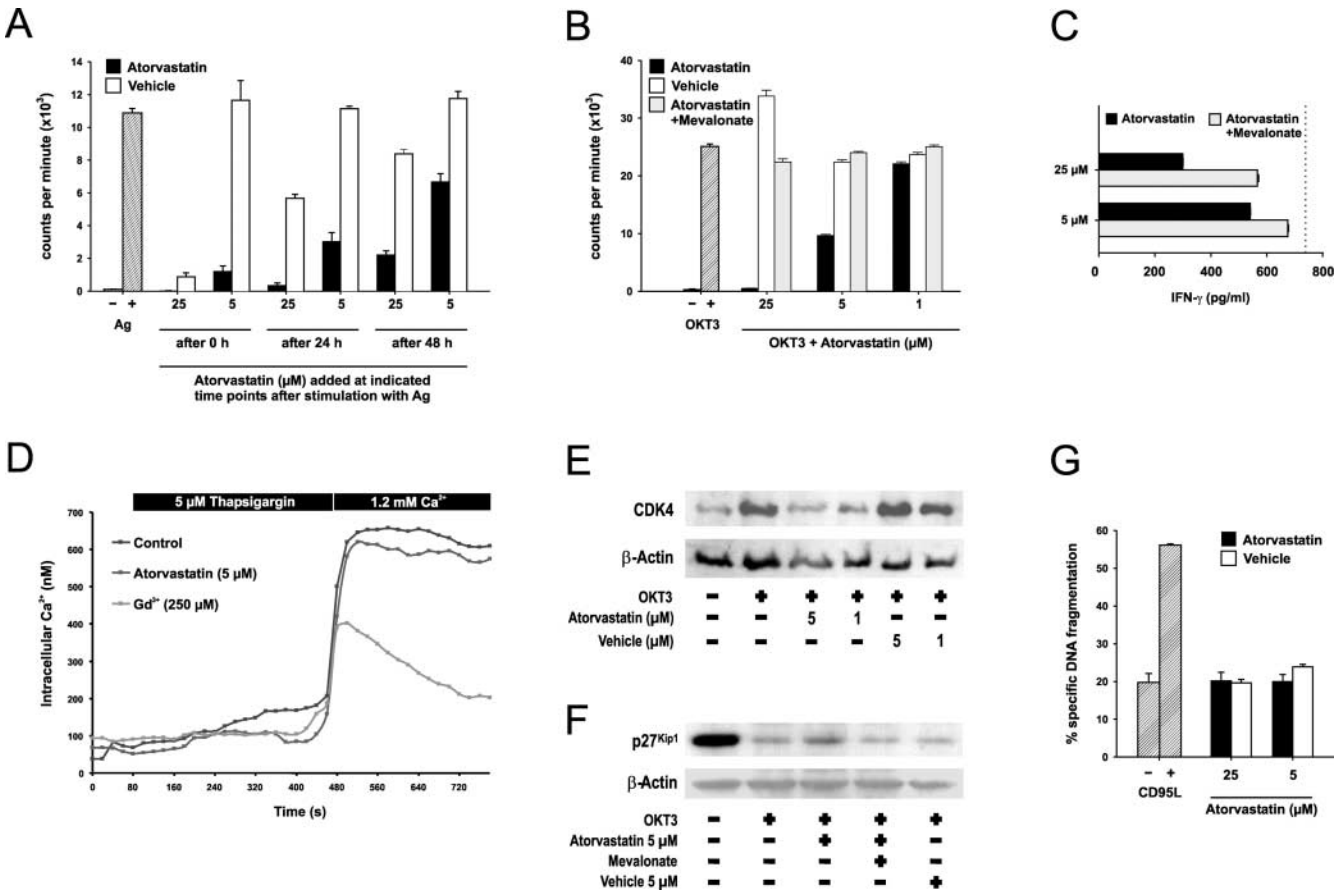

Figure 5. Pathways used by atorvastatin to interfere with T cell cycle. Hatched bars (A and B) correspond to controls without atorvastatin, vehicle, or L-mevalonate. (A) The representative human BP-specific TCL MB7 was stimulated with (+) or without (−) antigen presented by irradiated autologous APC. Atorvastatin (shaded bars) or vehicle (open bars) was added immediately (0 h) or at later stages after 24 or 48 h, respectively. (B) MB7 was stimulated with (+) or without (−) anti-CD3/CD28 in the presence or absence of atorvastatin or vehicle, respectively. Gray bars indicate the addition of L-mevalonate (200 μM). (C) Accordingly, IFN-γ was measured in the supernatant. The cytokine levels, derived from cells treated with (gray bars) or without (black bars) L-mevalonate, are given in relation to vehicle control (dotted line). (D) The representative MBP-specific TCL EG8 is demonstrated as an example for the measurement of Ca^{2+} influx by flow cytometry. Cells were incubated for 24 h in the absence (control) or presence of atorvastatin and Ca^{2+} influx was monitored by a Tg model of CRAC activation (Materials and Methods). Gd^{3+}, a Ca^{2+} entry blocker, was used as a positive control. (E) Expression of CDK4 was assessed 24 h after anti-CD3/CD28 stimulation of the representative MBP-specific TCL EG7 by immunoblotting. (F) MB7 was used to demonstrate the CDK inhibitor $p27^{kip1}$ regulation by atorvastatin and mevalonate blockade. (G) Jurkat T cells were incubated with (+) or without (−) 10 U/ml murine CD95 ligand as controls (hatched bars) or with the indicated concentrations of atorvastatin or vehicle, respectively. After 24 h, specific DNA fragmentation was measured by flow cytometry.

show that atorvastatin-induced up-regulation of $p27^{kip1}$ is blocked by L-mevalonate. Altogether, this pathway explains the down-regulation of CDK4 and up-regulation of $p27^{kip1}$ by atorvastatin.

Our data provide compelling evidence for the beneficial role of statins in neuroinflammation. In addition to the reported pleiotropic mechanisms exhibited by this group of substances, here we unravel the inhibition of HMG-CoA reductase as a responsible mechanism for the direct T cell–targeted influence of atorvastatin on proliferation and effector cytokines of Th1 cells. Due to the therapeutic potential of this pathway in EAE, the activity of statins might open up a new avenue for MS treatment with an orally administered drug.

We thank Michael Rupschus for technical assistance, Prof. Steffen Hauptmann (Charité) for technical support, Dr. Reinhard Geßner (Charité) for cholesterol analysis, Dr. Toralf Kaiser (Joint Flow Cytometry Core Facility of the Max-Planck-Institute for Infection Biology, German Rheumatism Research Center, and Charité) for assistance with calcium measurements, Dr. Julian Bösel and Dr. Karen Gertz for technical hints, and Celia Forbes for carefully reading the manuscript as a native speaker.

This work was supported by grants from the Bundesministerium für Bildung und Forschung to F. Zipp and S. Brocke, the Deutsche Forschungsgemeinschaft to F. Zipp and R. Nitsch (507), and to M. Endres (En343/7-1; 4-2; 6-2), the Hermann and Lilly-Schilling Foundation to M. Endres, and the Boehringer Ingelheim Fonds to O. Aktas.

Submitted: 15 August 2002
Revised: 6 January 2003
Accepted: 21 January 2003

Published March 10, 2003

References

1. Maron, D.J., S. Fazio, and M.F. Linton. 2000. Current perspectives on statins. *Circulation.* 101:207–213.
2. Albert, M.A., E. Danielson, N. Rifai, and P.M. Ridker. 2001. Effect of statin therapy on C-reactive protein levels: the pravastatin inflammation/CRP evaluation (PRINCE): a randomized trial and cohort study. *JAMA.* 286:64–70.
3. Ridker, P.M., N. Rifai, M. Clearfield, J.R. Downs, S.E. Weis, J.S. Miles, and A.M. Gotto. 2001. Measurement of C-reactive protein for the targeting of statin therapy in the primary prevention of acute coronary events. *N. Engl. J. Med.* 344:1959–1965.
4. Kobashigawa, J.A., S. Katznelson, H. Laks, J.A. Johnson, L. Yeatman, X.M. Wang, D. Chia, P.I. Terasaki, A. Sabad, G.A. Cogert, et al. 1995. Effect of pravastatin on outcomes after cardiac transplantation. *N. Engl. J. Med.* 333:621–627.
5. Kwak, B., F. Mulhaupt, S. Myit, and F. Mach. 2000. Statins as a newly recognized type of immunomodulator. *Nat. Med.* 6:1399–1402.
6. Weitz-Schmidt, G., K. Welzenbach, V. Brinkmann, T. Kamata, J. Kallen, C. Bruns, S. Cottens, Y. Takada, and U. Hommel. 2001. Statins selectively inhibit leukocyte function antigen-1 by binding to a novel regulatory integrin site. *Nat. Med.* 7:687–692.
7. Palinski, W. 2000. Immunomodulation: a new role for statins? *Nat. Med.* 6:1311–1312.
8. Miller, S.D., and W.J. Karpus. 1994. The immunopathogenesis and regulation of T cell-mediated demyelinating diseases. *Immunol. Today.* 15:356–361.
9. Raine, C.S., and U. Traugott. 1984. Experimental autoimmune demyelination. Chronic relapsing models and their therapeutic implications for multiple sclerosis. *Ann. NY Acad. Sci.* 436:33–51.
10. Zamvil, S.S., and L. Steinman. 1990. The T lymphocyte in experimental allergic encephalomyelitis. *Annu. Rev. Immunol.* 8:579–621.
11. Goverman, J., and T. Brabb. 1996. Rodent models of experimental allergic encephalomyelitis applied to the study of multiple sclerosis. *Lab. Anim. Sci.* 46:482–492.
12. Constantin, G., S. Brocke, A. Izikson, C. Laudanna, and E. Butcher. 1998. Tyrphostin AG490, a tyrosine kinase inhibitor, blocks actively induced experimental autoimmune encephalomyelitis. *Eur. J. Immunol.* 28:3523–3529.
13. Brocke, S., A. Gaur, C. Piercy, A. Gautam, K. Gijbels, C.G. Fathman, and L. Steinman. 1993. Induction of relapsing paralysis in experimental autoimmune encephalomyelitis by bacterial superantigen. *Nature.* 365:642–644.
14. Jansson, M., V. Panoutsakopoulu, J. Baker, L. Klein, and H. Cantor. 2002. Attenuated experimental autoimmune encephalomyelitis in eta-1/osteopontin-deficient mice. *J. Immunol.* 168:2096–2099.
15. Wendling, U., H. Walczak, J. Dörr, C. Jacobi, M. Weller, P.H. Krammer, and F. Zipp. 2000. Expression of TRAIL receptors in human autoreactive and foreign antigen-specific T cells. *Cell Death Differ.* 7:637–644.
16. Lünemann, J.D., S. Waiczies, S. Ehrlich, U. Wendling, B. Seeger, T. Kamradt, and F. Zipp. 2002. Death ligand TRAIL induces no apoptosis but inhibits activation of human (auto)antigen-specific T cells. *J. Immunol.* 168:4881–4888.
17. Brocke, S., L. Quigley, H.F. McFarland, and L. Steinman. 1996. Isolation and characterization of autoreactive T cells in experimental autoimmune encephalomyelitis of the mouse. *Methods Enzymol.* 9:458–462.
18. Griffioen, A.W., G.T. Rijkers, J. Keij, and B.J. Zegers. 1989. Measurement of cytoplasmic calcium in lymphocytes using flow cytometry. Kinetic studies and single cell analysis. *J. Immunol. Methods.* 120:23–27.
19. Smith, T., A. Groom, B. Zhu, and L. Turski. 2000. Autoimmune encephalomyelitis ameliorated by AMPA antagonists. *Nat. Med.* 6:62–66.
20. Vanderlugt, C.L., S.M. Rahbe, P.J. Elliott, M.C. Dal Canto, and S.D. Miller. 2000. Treatment of established relapsing experimental autoimmune encephalomyelitis with the proteasome inhibitor PS-519. *J. Autoimmun.* 14:205–211.
21. Bisgaier, C.L., A.D. Essenburg, B.J. Auerbach, M.E. Pape, C.S. Sekerke, A. Gee, S. Wolle, and R.S. Newton. 1997. Attenuation of plasma low density lipoprotein cholesterol by select 3-hydroxy-3-methylglutaryl coenzyme A reductase inhibitors in mice devoid of low density lipoprotein receptors. *J. Lipid Res.* 38:2502–2515.
22. Johnston, T.P., L.B. Nguyen, W.A. Chu, and S. Shefer. 2001. Potency of select statin drugs in a new mouse model of hyperlipidemia and atherosclerosis. *Int. J. Pharm.* 229:75–86.
23. van de Poll, S.W., T.J. Romer, O.L. Volger, D.J. Delsing, T.C. Bakker Schut, H.M. Princen, L.M. Havekes, J.W. Jukema, A. van der Laarse, and G.J. Puppels. 2001. Raman spectroscopic evaluation of the effects of diet and lipid-lowering therapy on atherosclerotic plaque development in mice. *Arterioscler. Thromb. Vasc. Biol.* 21:1630–1635.
24. Endres, M., U. Laufs, Z. Huang, T. Nakamura, P. Huang, M.A. Moskowitz, and J.K. Liao. 1998. Stroke protection by 3-hydroxy-3-methylglutaryl (HMG)-CoA reductase inhibitors mediated by endothelial nitric oxide synthase. *Proc. Natl. Acad. Sci. USA.* 95:8880–8885.
25. Laufs, U., K. Gertz, P. Huang, G. Nickenig, M. Bohm, U. Dirnagl, and M. Endres. 2000. Atorvastatin upregulates type III nitric oxide synthase in thrombocytes, decreases platelet activation, and protects from cerebral ischemia in normocholesterolemic mice. *Stroke.* 31:2442–2449.
26. Boberg, M., R. Angerbauer, W.K. Kanhai, W. Karl, A. Kern, M. Radtke, and W. Steinke. 1997. Biotransformation of cerivastatin in mice, rats, and dogs in vivo. *Drug Metab. Dispos.* 26:640–652.
27. Bernini, F., A. Poli, and R. Paoletti. 2001. Safety of HMG-CoA reductase inhibitors: focus on atorvastatin. *Cardiovasc. Drugs Ther.* 15:211–218.
28. Black, A.E., M.W. Sinz, R.N. Hayes, and T.F. Woolf. 1998. Metabolism and excretion studies in mouse after single and multiple oral doses of the 3-hydroxy-3-methylglutaryl-CoA reductase inhibitor atorvastatin. *Drug Metab. Dispos.* 26:755–763.
29. Stern, R.H., B.B. Yang, N.J. Hounslow, M. MacMahon, R.B. Abel, and S.C. Olson. 2000. Pharmacodynamics and pharmacokinetic-pharmacodynamic relationships of atorvastatin, an HMG-CoA reductase inhibitor. *J. Clin. Pharmacol.* 40:616–623.
30. Panitch, H., R.L. Hirsch, J. Schindler, and K.P. Johnson. 1987. Treatment of multiple sclerosis with gamma interferon: exacerbations associated with activation of the immune system. *Neurology.* 37:1097–1102.
31. Tran, E.H., E.N. Prince, and T. Owens. 2000. IFN-gamma shapes immune invasion of the central nervous system via regulation of chemokines. *J. Immunol.* 164:2759–2768.
32. Tanuma, N., T. Shin, K. Kogure, and Y. Matsumoto. 1999. Differential role of TNF-alpha and IFN-gamma in the brain

of rats with chronic relapsing autoimmune encephalomyelitis. *J. Neuroimmunol.* 96:73–79.

33. Lea, A.P., and D. McTavish. 1997. Atorvastatin. A review of its pharmacology and therapeutic potential in the management of hyperlipidaemias. *Drugs.* 53:828–847.
34. Chirathaworn, C., J.E. Kohlmeier, S.A. Tibbetts, L.M. Rumsey, M.A. Chan, and S.H. Benedict. 2002. Stimulation through intercellular adhesion molecule-1 provides a second signal for T cell activation. *J. Immunol.* 168:5530–5537.
35. Stanislaus, R., A.K. Singh, and I. Singh. 2001. Lovastatin treatment decreases mononuclear cell infiltration into the CNS of Lewis rats with experimental allergic encephalomyelitis. *J. Neurosci. Res.* 66:155–162.
36. Liao, J.K. 2002. Isoprenoids as mediators of the biological effects of statins. *J. Clin. Invest.* 110:285–288.
37. Blanco-Colio, L.M., A. Villa, M. Ortego, M.A. Hernandez-Presa, A. Pascual, J.J. Plaza, and J. Egido. 2002. 3-Hydroxy-3-methyl-glutaryl coenzyme A reductase inhibitors, atorvastatin and simvastatin, induce apoptosis of vascular smooth muscle cells by downregulation of Bcl-2 expression and Rho A prenylation. *Atherosclerosis.* 161:17–26.
38. Youssef, S., O. Stüve, J.C. Patarroyo, P.J. Ruiz, J.L. Radosevich, E.M. Hur, M. Bravo, D.J. Mitchell, R.A. Sobel, L. Steinman, and S.S. Zamvil. 2002. The HMG-CoA reductase inhibitor, atorvastatin, promotes a Th2 bias and reverses paralysis in central nervous system autoimmune disease. *Nature.* 420:78–84.
39. Naderi, S., R. Blomhoff, J. Myklebust, E.B. Smeland, B. Erikstein, K.R. Norum, and H.K. Blomhoff. 1999. Lovastatin inhibits G1/S transition of normal human B-lymphocytes independent of apoptosis. *Exp. Cell Res.* 252:144–153.
40. Danesh, F.R., M.M. Sadeghi, N. Amro, C. Philips, L. Zeng, S. Lin, A. Sahai, and Y.S. Kanwar. 2002. 3-Hydroxy-3-methylglutaryl CoA reductase inhibitors prevent high glucose-induced proliferation of mesangial cells via modulation of Rho GTPase/ p21 signaling pathway: implications for diabetic nephropathy. *Proc. Natl. Acad. Sci. USA.* 99:8301–8305.
41. Hughes, D.A. 1995. Control of signal transduction and morphogenesis by Ras. *Semin. Cell Biol.* 6:89–94.
42. Hengst, L., and S.I. Reed. 1996. Translational control of p27Kip1 accumulation during the cell cycle. *Science.* 271: 1861–1864.

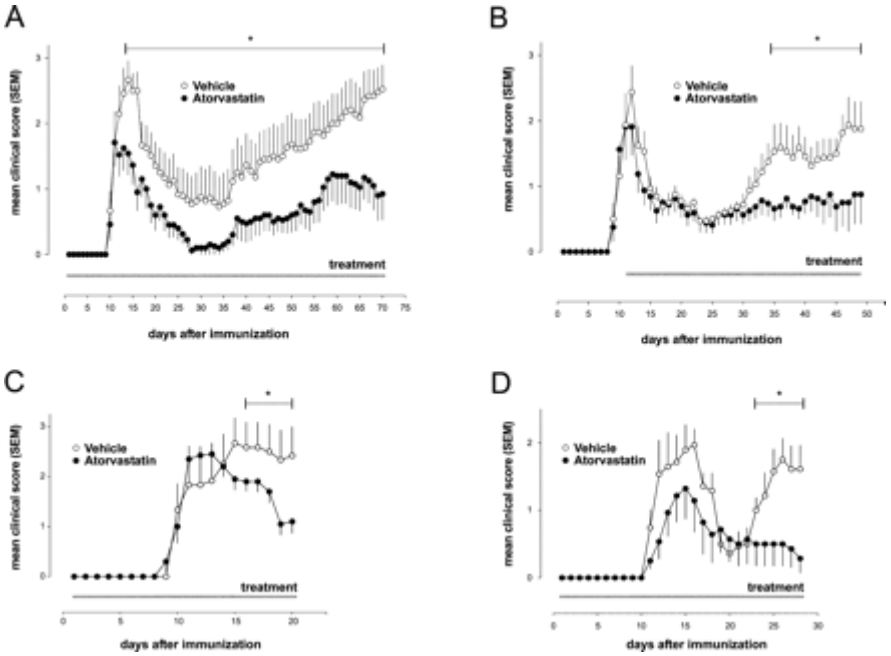

Figure 1.

Atorvastatin suppresses the clinical severity of EAE in a preventive and therapeutic manner. (A) For the preventive treatment paradigm, 200 μg atorvastatin (*n* = 12; shaded circles) or vehicle alone (*n* = 12; open circles) were injected subcutaneously daily from the day of immunization onward. Both the maximum disease scores and the mean clinical disease scores were significantly reduced in the atorvastatin group. (B) For the nonpreventive therapy, mice were randomized into two groups (*n* = 8 for both groups) after the establishment of disease at day 10 and subsequently treated. Significant differences were noted for the maximum disease scores, the relapse incidence, and the mean disease scores for the time of the relapse. (C) Mice were treated subcutaneously with 20 μg atorvastatin (*n* = 10 for atorvastatin group, *n* = 7 for vehicle group). (D) For oral therapy, mice were treated with 200 μg (*n* = 7 for both groups). For all trials, treatment periods are indicated by horizontal hatched bars. The treatment effect was statistically significant as outlined in the marked range for all presented EAE courses (*, $P < 0.05$, analysis of variance).

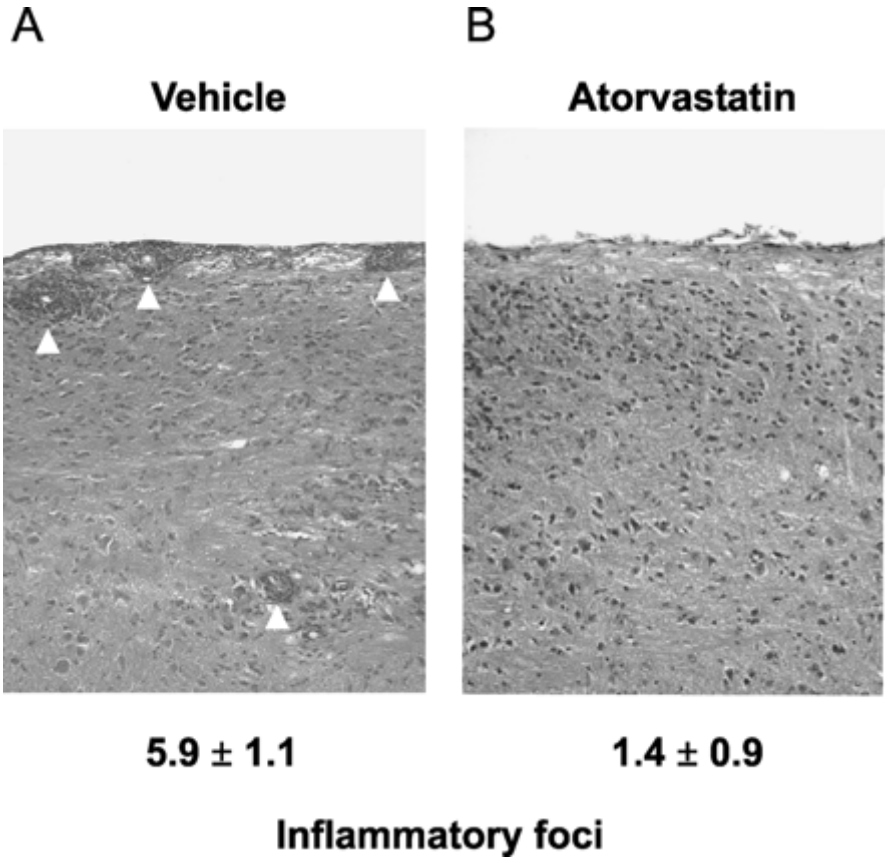

Figure 2.

Decreased inflammation in spinal cords of atorvastatin-treated mice. Representative histology of spinal cord longitudinal sections was obtained from the EAE course presented in Fig. 1 A. Inflammatory infiltration was visualized by hematoxylin and eosin staining. (A) Vehicle-treated animals showed typical perivascular infiltrates (arrowheads) comprised of lymphocytes and macrophages. (B) In contrast, atorvastatin-treated animals showed a markedly reduced inflammatory reaction. Average number of inflammatory foci/ocular field ± SEM in spinal cords of atorvastatin- and vehicle-treated mice as detected in hematoxylin and eosin–stained sections ($P < 0.01$, Student's *t* test).

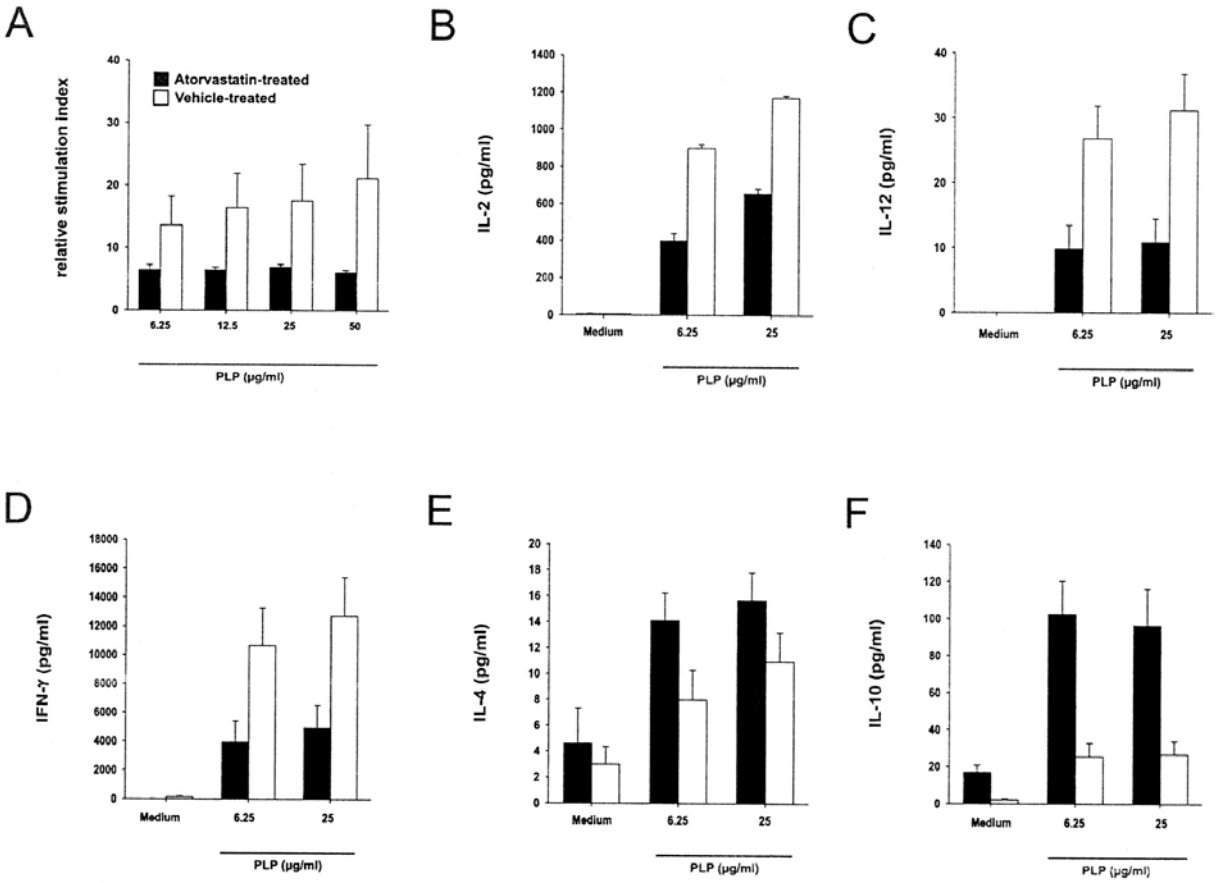

Figure 3.

Atorvastatin treatment in vivo suppresses the PLP-specific priming response. Three mice per group were treated with either atorvastatin (200 µg per mouse) or vehicle from day 1 after immunization with PLP as described in Materials and Methods. (A) Proliferation of splenocytes in response to PLP (at the indicated concentrations) was assessed in quadruplicate cultures and expressed as stimulation index (mean ± SEM; atorvastatin, shaded bars; vehicle, open bars). (B) Accordingly, IL-2 was determined in the supernatants. Whereas IL-12 (C) as well as IFN-γ (D) were found at lower concentrations in the atorvastatin-treated mice than in those vehicle-treated, levels of IL-4 (E) and IL-10 (F) were higher in supernatants from splenocytes after treatment with atorvastatin. Data are presented as mean ± SEM; differences between atorvastatin and vehicle treatment are significant ($P < 0.05$; Student's *t* test).

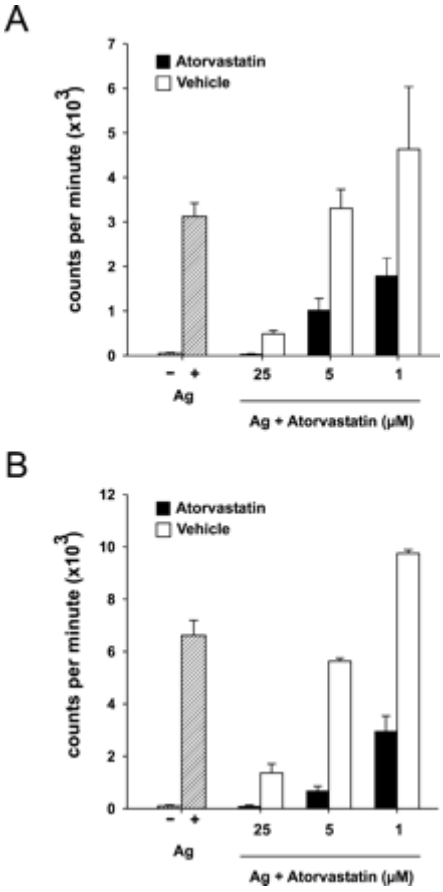

Figure 4.

Atorvastatin inhibits antigen-dependent proliferation of murine and human TCLs. The murine $CD4^+$ PLP-specific TCL Je1 (A) and the human BP-specific TCL MB8 (B) were stimulated with (+) or without (−) antigen presented by irradiated autologous APC in the absence or presence of different concentrations of atorvastatin (shaded bars) or vehicle alone (open bars), and proliferation was assessed. Striped bars correspond to controls without atorvastin or vehicle.

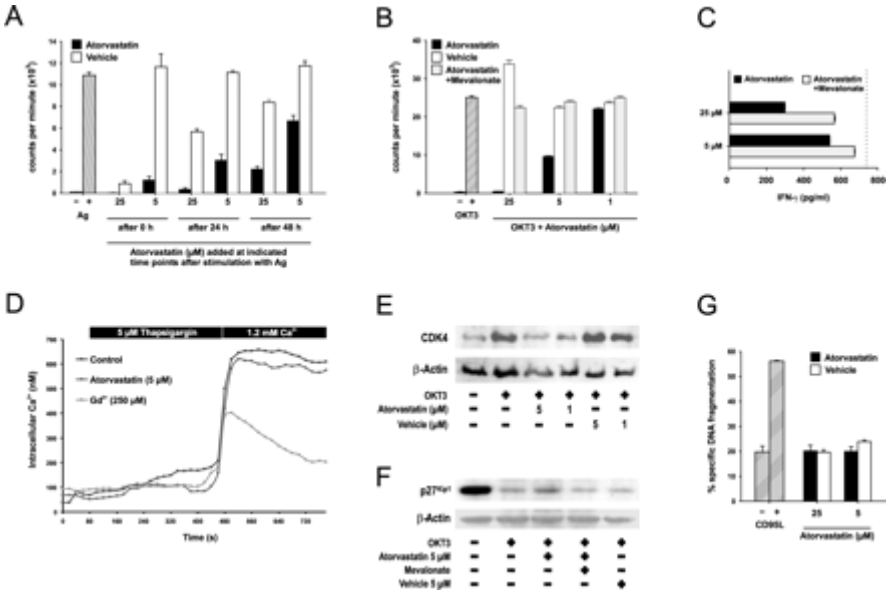

Figure 5.

Pathways used by atorvastatin to interfere with T cell cycle. Hatched bars (A and B) correspond to controls without atorvastatin, vehicle, or l-mevalonate. (A) The representative human BP-specific TCL MB7 was stimulated with (+) or without (−) antigen presented by irradiated autologous APC. Atorvastatin (shaded bars) or vehicle (open bars) was added immediately (0 h) or at later stages after 24 or 48 h, respectively. (B) MB7 was stimulated with (+) or without (−) anti-CD3/CD28 in the presence or absence of atorvastatin or vehicle, respectively. Gray bars indicate the addition of l-mevalonate (200 μM). (C) Accordingly, IFN-γ was measured in the supernatant. The cytokine levels, derived from cells treated with (gray bars) or without (black bars) l-mevalonate, are given in relation to vehicle control (dotted line). (D) The representative MBP-specific TCL EG8 is demonstrated as an example for the measurement of Ca^{2+} influx by flow cytometry. Cells were incubated for 24 h in the absence (control) or presence of atorvastatin and Ca^{2+} influx was monitored by a Tg model of CRAC activation (Materials and Methods). Gd^{3+}, a Ca^{2+} entry blocker, was used as a positive control. (E) Expression of CDK4 was assessed 24 h after anti-CD3/CD28 stimulation of the representative MBP-specific TCL EG7 by immunoblotting. (F) MB7 was used to demonstrate the CDK inhibitor $p27^{kip1}$ regulation by atorvastatin and mevalonate blockade. (G) Jurkat T cells were incubated with (+) or without (−) 10 U/ml murine CD95 ligand as controls (hatched bars) or with the indicated concentrations of atorvastatin or vehicle, respectively. After 24 h, specific DNA fragmentation was measured by flow cytometry.